ELSEVIER

Thermochimica Acta 383 (2002) 59–67

thermochimica
acta

www.elsevier.com/locate/tca

Thermal and spectral studies of binary complexes of cyanodithioformate with transition metal ions

Rajendra Prasad*, Azad Kumar

Department of Chemistry, University of Roorkee, Roorkee 247667, India

Received 6 January 2001; received in revised form 10 May 2001; accepted 25 June 2001

Abstract

Binary complexes of the type $[M(S_2CCN)_2]$ ($M = Mn^{2+}, Fe^{2+}, Co^{2+}, Ni^{2+}, Cu^{2+}$ and Zn^{2+}) have been synthesised from alcoholic solutions. They have been characterised using elemental analyses, IR, UV–VIS spectroscopy, magnetic susceptibility measurement and solution conductance data. In thermogravimetry (TG) studies, all these complexes exhibit a prominent weight loss step between 100 and 330 °C under a N_2 atmosphere. Besides, a second weight loss step has also been observed beyond 800° C for the Mn^{2+}, Fe^{2+} and Co^{2+} complexes, between 400 and 600 °C for Zn^{2+} complex and beyond 380 °C for Cu^{2+} complex. Broad differential thermal analysis (DTA) endotherms are observed corresponding to these weight loss steps. The first weight loss in the TG scan of the complexes follows a deceleratiory α–time curve with D_3 mechanism for all complexes. The activation energy (E_a) for the thermal decomposition varies between 43 and 115 kJ/mol and removal of CS_2 and/or CS have been suggested. Various decomposition parameters have been calculated.

Keywords: Cyanodithioformate; Synthesis; Thermogravimetry; Thermal degradation; Transition metal ion

1. Introduction

The chemical, spectral and thermal decomposition studies of cyanodithioformate (S_2CCN^-) ion and its complexes have been the least explored ones among the dithioacid family [1–5]. Although thermal decomposition parameters for various thioacid complexes have been reported, very little work has been done on S_2CCN^- [6–8]. Unlike the dithioformates and xanthates, the cyanodithioformate anion exhibits a very high proclivity for dimerisation through the removal of one ‘S’ atom per ion. Also, its alkali metal salts decompose spontaneously in dry state. However, it is very stable in the complexed state [4,5] as well as the $(NEt_4)^+$ salt.

The present paper reports the synthesis, spectral and thermal decomposition studies of a series of binary complexes of cyanodithioformate with bivalent transition metal ions (Structure **I**). Kinetic and thermal decomposition parameters have been calculated using the Freeman and Carrol method. Mechanistic models have been ascertained from the dα/dt versus T plots and the assigned ones are those that gave the best linear fit in the Arrhenius plots. The study shows that the solid state decomposition of S_2CCN^- complexes do not follow the dimerisation path as exhibited by the ion in solutions.

---

* Corresponding author. Fax: +91-1332-73560.
E-mail address: rajenfcy@rurkiu.ernet.in (R. Prasad).

0040-6031/02/$ – see front matter
PII: S0040-6031(01)00656-6

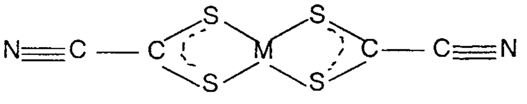

1: M = Mn^{2+} 2: M = Fe^{2+}
3: M = Co^{2+} 4: M = Ni^{2+}
5: M = Cu^{2+} 6: M = Zn^{2+}

2. Experimental

Na_2S_2CCN.3dmf compound was prepared according to the literature procedure [9]. Solvents were dried before use. AR grade sulphate salts of manganese(II), iron(II), nickel(II) and copper(II) and chlorides of cobalt(II) and zinc(II) were used. Solutions for metal estimations were prepared by NaOH–$NaNO_3$ fusion method while that for sulphur estimations were prepared by treating with concentrated bromine solutions followed by repeated treatment with conc. HNO_3 [10]. C and N analyses were obtained from RSIC–CDRI, Lucknow. IR spectra were recorded on a Perkin-Elmer 1600 FTIR spectrophotometer with KBr pellets, electronic spectra on a Schimadzu-1601 spectrophotometer with nujol thin films. Magnetic susceptibilities were measured on a PARC-155 Magnetometer at 25 °C. Thermogravimetry/differential thermal analysis (TG/DTA) experiments were carried out on a Stanton Redcroft Thermobalance STA-780 under a dynamic N_2 atmosphere at a flow rate of 50 ml/min and heating rate 10 °C/min. Computations were carried out using a series of BASIC programs.

2.1. Preparation of the complexes

The complexes were prepared using a general procedure as follows. A suspension of finely powdered metal salts (4.0 mmol) and freshly prepared Na_2S_2CCN.3dmf (4.0 g, ca. 10 mmol) in dry EtOH (100 ml) was stirred for 4–6 h at 40 °C under a N_2 atmosphere. For iron, nickel and copper salts, brown-coloured compounds and for manganese and zinc yellowish-white compounds separated out. For the cobalt salt, the reaction mixture yielded a green solution which was filtered, and the solvent removed from the filtrate at reduced pressure. The residue was collected. The solids thus obtained were washed twice with water followed by EtOH and Et_2O. The compounds were recrystallised from acetone–Et_2O mixture and dried over $CaCl_2$. Yield: ca. 0.40–0.75 g (38–71%).

3. Results and discussions

Reaction between metal salts and Na_2S_2CCN.3dmf in 2:5 molar ratio in absolute ethanol have yielded bis-chelate complexes of the type $M(S_2CCN)_2$. The ligand has a tendency to undergo dimerisation reaction in water and chloroform, but not in dry alcohol. Although hydrated metal salts have been used in these syntheses, the traces of water does not cause dimerisation to any significant extent, as the formation of corresponding maleonitriledithiolate complexes as side reaction products has not been observed [11,12]. The complexes have been characterised using elemental analyses and spectral data (Table 1). All these complexes are insoluble in water and only moderately soluble in acetone, acetonitrile, DMF and DMSO and other polar organic solvents. Conductance measurements of their acetonitrile solutions indicate non-electrolyte nature. All except nickel and zinc complexes are air sensitive.

Complexes even upon prolonged refluxing in water do not liberate sulphur nor disproportionate to form anionic maleonitriledithiolate complexes. This is indicative of the marked stabilisation of the anion upon its co-ordination. However, upon treatment with benzyl chloride in boiling ethanol, complexes dissociate giving metal halides and the pale yellow solution of benzyl cyanodithioformate.

3.1. IR spectra

IR spectra of the complexes indicates (η^2-S,S') co-ordination. There are two characteristic group frequencies [5], namely, ν(CN) and $\nu(-\mathrm{C}{<}^{S}_{S})$, of which the $\nu(-\mathrm{C}{<}^{S}_{S})$ is quite sensitive of the co-ordination mode. In the case of η^1-S co-ordination, two bands are observed between 1100 and 1000 cm^{-1} due to $-\mathrm{C}{<}^{S}_{S}$ group, which are assigned to ν_{as}(C–S) and ν_s(C=S) stretching frequencies [1,4,5]. However, in the case of (η^2-S,S') co-ordination, the $\nu(-\mathrm{C}{<}^{S}_{S})$ group vibration resolves into symmetric and anti-symmetric modes of which the anti-symmetric mode is observed between 1100 and 1000 cm^{-1} and the symmetric mode between 600 and 700 cm^{-1} [13,14].

Table 1
Analytical magnetic and spectral data[a]

Complex	Analyses found (calcd.) (%)				μ_{eff} (BM)	IR (cm^{-1})			Electronic (λ_{max}/nm)
	C	N	S	M		ν(CN)	$\nu_{as}(CS_2)$	$\nu_s(CS_2)$	
$[Mn(S_2CCN)_2]$	18.1 (18.5)	10.0 (10.8)	48.0 (49.4)	20.5 (21.2)	0.197	2190	1023	625	336, 278(sh), 229
$[Fe(S_2CCN)_2]$	18.2 (18.5)	10.1 (10.8)	48.0 (49.2)	21.0 (21.5)	0.269	2235	1010	625	852(w), 359, 223, 280
$[Co(S_2CCN)_2]$	17.9 (18.3)	10.4 (10.7)	48.7 (48.7)	22.4 (22.4)	0.037	2220	1020	630	278(sh), 258, 226
$[Ni(S_2CCN)_2]$	18.5 (18.3)	10.2 (10.7)	48.7 (48.7)	22.8 (22.3)	0.072	2215	1000	630	500(vw), 273, 223
$[Cu(S_2CCN)_2]$	17.6 (17.9)	10.0 (10.5)	47.5 (47.9)	23.2 (23.7)	0.042	2220	995	620	630, 467, 254, 223
$[Zn(S_2CCN)_2]$	17.5 (17.8)	10.0 (10.4)	47.2 (47.5)	24.2 (24.2)	–	2210	1000	620	385, 265, 223

[a] At 298 K, as thin film of paste in nujol; w: weak; vw: very weak.

All complexes exhibit a band between 2200 and 2235 cm^{-1} due to ν(C=N) stretching vibration, which is observed at 20–55 cm^{-1} higher frequency than that in uncoordinated ligand. This behaviour is contrary to what is expected from the π back-donation effect. The higher frequency side shift of the ν(CN) band seems to arise from coupling of the stretching frequencies of the two juxtaposed CN groups into symmetric and antisymmetric modes. In these complexes, the two CN groups are linearly arranged. The ν_{as}(CN) being IR active is more likely to be observed at higher frequency than that in free ligand. The magnitude of the shift decreases, on going from iron through zinc metal ion, and is in agreement with metal ligand π back-donation. Unlike the poor π acidity of xanthates and dithiocarbamates, the cyanodithioformate is a good π acid. The difference lies in the nature of the π function of the cyanodithioformate vis-à-vis other dithioacids. In cyanodithioformate, the π functions of the 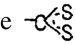 group interact with the p–π orbitals of the CN group. Thereby, five π molecular orbitals are generated of which only three are occupied. Contrary to this in xanthates and dithiocarbamates, the π function of the  group couples with only one p–π orbital bearing a lone pair on the O/N atom. Thus, out of the four π molecular orbitals, three are occupied [15]. The symmetry and energy of the ψ_4 function in cyanodithioformate is favourable for strong π interaction with metal ions causing a decrease in the CN bond order.

3.2. Magnetic properties

The magnetic moments of the solid samples were measured at ambient temperature (25 °C) and the observed values are listed in Table 1. It can be seen that these values are invariably lower than those the ones expected in high spin configurations. Literature evidences suggest that bivalent manganese [16], iron [17], cobalt [18] and copper [19] complexes with xanthates and dithiocarbamates exhibit antiferromagnetic coupling. Thus, the observed lower magnetic moments for the analogous S_2CCN^- complexes are not unreasonable. The $[Ni(S_2CCN)_2]$ is expected to possess square planar arrangement of donor ‘S’ atoms [20] and hence is diamagnetic.

3.3. Electronic spectra

The prominent bands observed in the UV–VIS spectra of these complexes are listed in Table 1. Due to the poor solubility of these complexes, it is likely that the d–d bands were not observed. However, it is also possible that they lie in the NIR region. In order to increase concentrations, the spectra were recorded in thin films consisting of nujol pastes of the compounds. The bands observed in the UV-region primarily originate from n → π* and π → π* intraligand transitions [4,5,15]. These bands are sensitive to the nature of metal ion and thus indicate strong π back-interactions. However, any definite trend could not be deduced from these shifts.

3.4. Thermal studies

The TG and DTA of the compounds were recorded under a dynamic N_2 atmosphere and some of the important characteristics are listed in Table 2.

All complexes, except the Ni^{2+} complex, decompose in two steps. The first step occurs between 65 and

Table 2
TG, DTA characteristics of the complexes[a]

Complex	Decomposition temperature (°C)		Product expected		Residue at (330 °C)		DTA endotherms		Phase change in residue
	T_i	T_f	Nature	Mass expected (calcd.) (%)	Nature	Mass expected (calcd.) (%)	Melting	Decomposition	
$[Mn(S_2CCN)_2]$	100	330	C_3S_2	38.4(38.6)	Mn(SCN)(NS)	61.6(61.4)	91 sh(w)	36–285	790 br(w)
$[Fe(S_2CCN)_2]$	190	330	CS_2	30.4(29.2)	$Fe(CN)(S_2CCN)$	69.6(70.8)	97 br(w)	36–300	812 sh(vs)
$[Co(S_2CCN)_2]$	185	320	CS_2	30.4(28.9)	$Co(CN)(S_2CCN)$	69.6(71.1)	97 sh(w)	36–285	814 sh(vs)
$[Ni(S_2CCN)_2]$	155	290	CS_2	26.4(28.9)	$Ni(CN)(S_2CCN)$	73.6(71.1)	91 sh(w)	36–290	903 sh(vs)
$[Cu(S_2CCN)_2]$	100	310	C_3S_2, CS	45.6(44.9)	Cu(CN)(SCN)	54.4(55.1)	90 br(w)	36–285	–
$[Zn(S_2CCN)_2]$	65	300	CS_2	27.6(28.2)	$Zn(CN)(S_2CCN)$	72.4(71.8)	91 sh(w)	36–260	878 sh

[a] br: broad; sh: sharp; vs: very strong; w: weak.

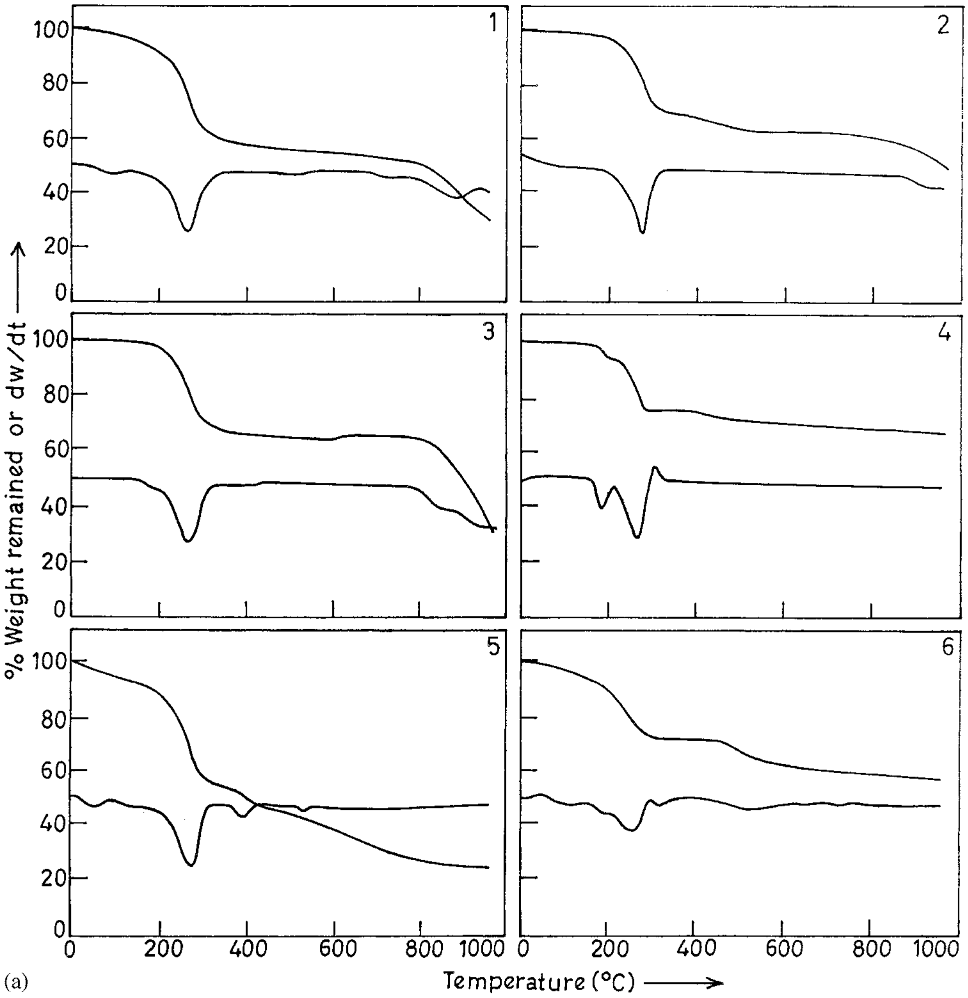

Fig. 1. (a) TG and DTG curves of complexes 1–6. (b) DTA curves of complexes 1–6.

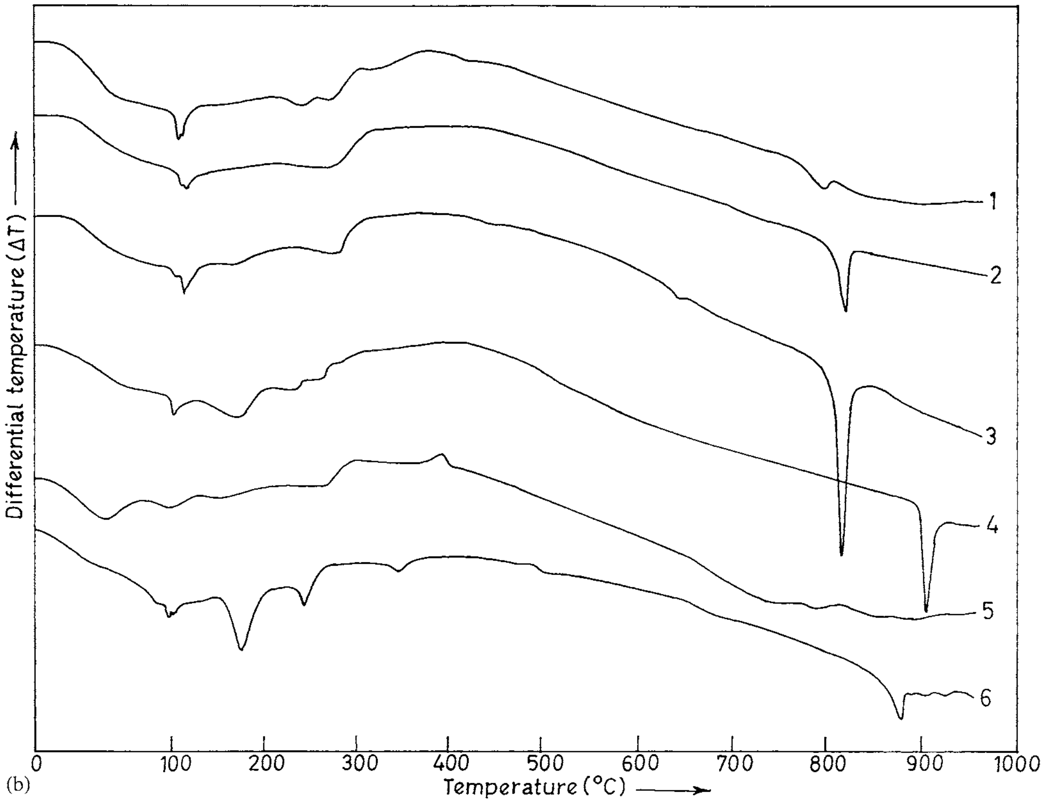

Fig. 1. (*Continued*).

330 °C and brings about 25–45% mass loss, depending upon the nature of the metal ion (Fig. 1a). This loss corresponds to the loss of a CS_2 molecule. However, in the case of Mn^{2+}, this loss corresponds to C_3S_2, and for Cu^{2+} complex to both CS_2 and CS. The second mass loss occurs beyond 800 °C for Mn, Fe and Co complexes and between 400 and 600 °C for the zinc complex. The copper complex exhibits a second gradual mass loss beyond 380 °C. The nickel complex exhibits two closely spaced mass loss steps between 155 and 210 °C (ca. 5% weight loss) and 210 and 300 °C ((ca. 21.4% weight loss) and there after no mass loss step until 950 °C. The second mass losses possibly result into the formation of metal nitrides. All these mass loss steps correspond to broad endotherms in the DTA curves (Fig. 1b). The first stage decomposition products of iron, cobalt, nickel and zinc complexes undergo a phase transition between 800 and 900 °C, seen as a sharp endotherm in the DTA scans.

The Freeman and Carrol method [21] was used to evaluate the kinetic parameters from the steep part of the TG curves, i.e. between 195 and 315 °C for Mn^{2+}, Fe^{2+}, Co^{2+} and Cu^{2+}, 210 and 290 °C for Ni^{2+} and 175 and 290 °C for Zn^{2+} complexes. The plots of $\Delta\ln(\mathrm{d}w/\mathrm{d}t)/\Delta\ln(wr)$ versus $\Delta(1/T)/\Delta\ln(wr)$ (where $\Delta\ln(\mathrm{d}w/\mathrm{d}t) = \ln(\mathrm{d}w/\mathrm{d}t)_T - \ln(\mathrm{d}w/\mathrm{d}t)_{T_{10}}$, $\Delta(1/T) = (1/T) - (1/T_{10})$, $\Delta\ln(wr)_T - \ln(wr)_{T_{10}}$) for different stages of the thermal decompositions are given in Fig. 2. The frequency factor ($\ln A$) for the decomposition processes were calculated using the following relationship:

$$\ln\left[\frac{(\mathrm{d}\alpha/\mathrm{d}t)}{(1-\alpha)^n}\right] = \ln A - \frac{E_\mathrm{a}}{RT} \qquad (1)$$

where $(\mathrm{d}\alpha/\mathrm{d}t) = (\mathrm{d}\alpha/\mathrm{d}T)^{*}\phi$, α is fraction decomposed, ϕ the heating rate and n the order of decomposition reaction which was obtained from Fig. 2.

The T_i, T_{10} and T_f (initial temperature, temperature for 10% and temperature for maximum mass loss for

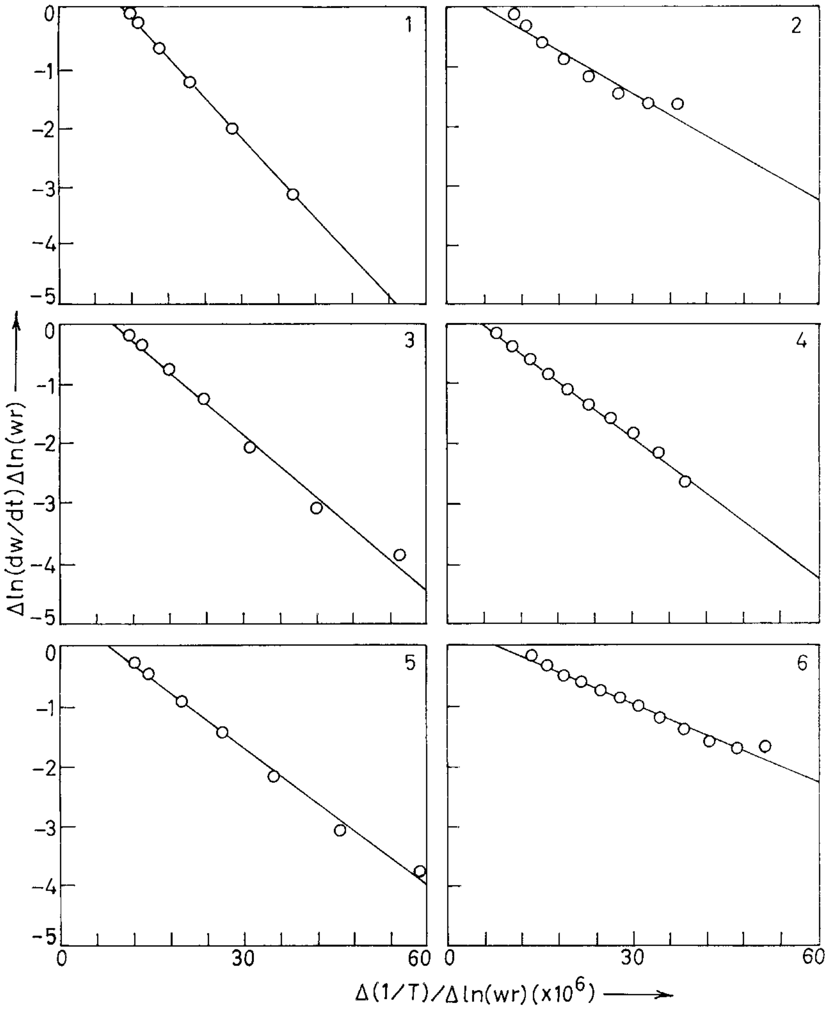

Fig. 2. Plots of $\Delta \ln(dw/dt)/\Delta \ln(wr)$ vs. $\Delta(1/T)/\Delta \ln(wr)$ for the first step for complexes 1–6.

first step), T_p (temperature for maximum rate of mass loss) have been used as the main criteria to indicate the thermal stability of the complexes. Form the T_{10} and T_p value, the stability order of the complexes could be given as Zn < Cu < Ni $\simeq$ Mn < Fe $\simeq$ Co.

The T_{10}, T_{90}, T_p (temperatures for 10 and 90% decompositions and that for highest decomposition rate), α_{max} (fraction decomposed at maximum decomposition rate), $(d\alpha/dt)_{max}$, activation energy (E_a) and frequency factor (A), are given in Table 3. The activation energy (E_a) and frequency factor were also calculated using the mechanistic models based on the differential forms of the kinetic equations [22]. These mechanistic models were assigned on the basis of the DTG characteristics of the thermal decompositions (Fig. 3) vis-à-vis the Arrhenius plots that gave the best linear fit. Although, from the DTG characteristics the Mn^{2+} and Co^{2+} complexes seem to follow Prout–Tomkins (B_1) mechanism, this gives unusually low values for $\ln A$ (−1.10, −0.39) and E_a (14.9 and 179.9 kJ/mol, respectively). Instead, the first-order (F_1) mechanism for Co^{2+} complex gives reasonable values ($\ln A = 15.40$, $E_a = 91.6$ kJ/mol). The values for the D_3 mechanism are given in Table 3 for all complexes. The mechanistic model-based E_a and $\ln A$ values for all complexes are comparatively much

Table 3
Data obtained from TG and DTG analysis: temperature characteristics, fraction decomposed at highest decomposition rate, maximum rate of decomposition, half width of DTG curve and kinetic parameters[a]

Complex	Temperatures (K)			α_{max}	$(d\alpha/dt)_{max}$ $\times 10^2$	Half width	Mechanistic parameters[b]			Freeman and Carrol parameters		
	T_{10}	T_{90}	T_p				Model	E_a (kJ/mol)	ln *A* (s)	Order	E_a (kJ/mol)	ln *A* (s)[c]
[Mn($S_2CCN)_2$]	495	566	538	0.556	1.56	46	D3	169.8	31.40	1.314	115.3	21.04
[Fe($S_2CCN)_2$]	496	562	543	0.624	1.85	37	D3	163.4	29.94	0.479	61.4	8.10
[Co($S_2CCN)_2$]	496	563	533	0.508	1.53	62	D3	182.2	34.30	0.841	87.6	14.40
[Ni($S_2CCN)_2$]	502	550	539	0.683	2.13	47	D3	220.3	43.55	0.462	76.1	11.80
[Cu($S_2CCN)_2$]	496	563	544	0.644	1.57	50	D3	167.1	30.81	0.660	76.8	11.70
[Zn($S_2CCN)_2$]	466	543	525	0.690	1.33	54	D3	124.4	22.43	0.380	43.1	4.22

[a] T_p: temperature at which ($d\alpha/dt$) is maximum.

[b] Mechanistic models (D3: three-dimensional diffusion with deceleratiory α–time curve).

[c] Calculated from $\ln[(d\alpha/dt)/(1-\alpha)^n]$ vs. $1/T$ plot.

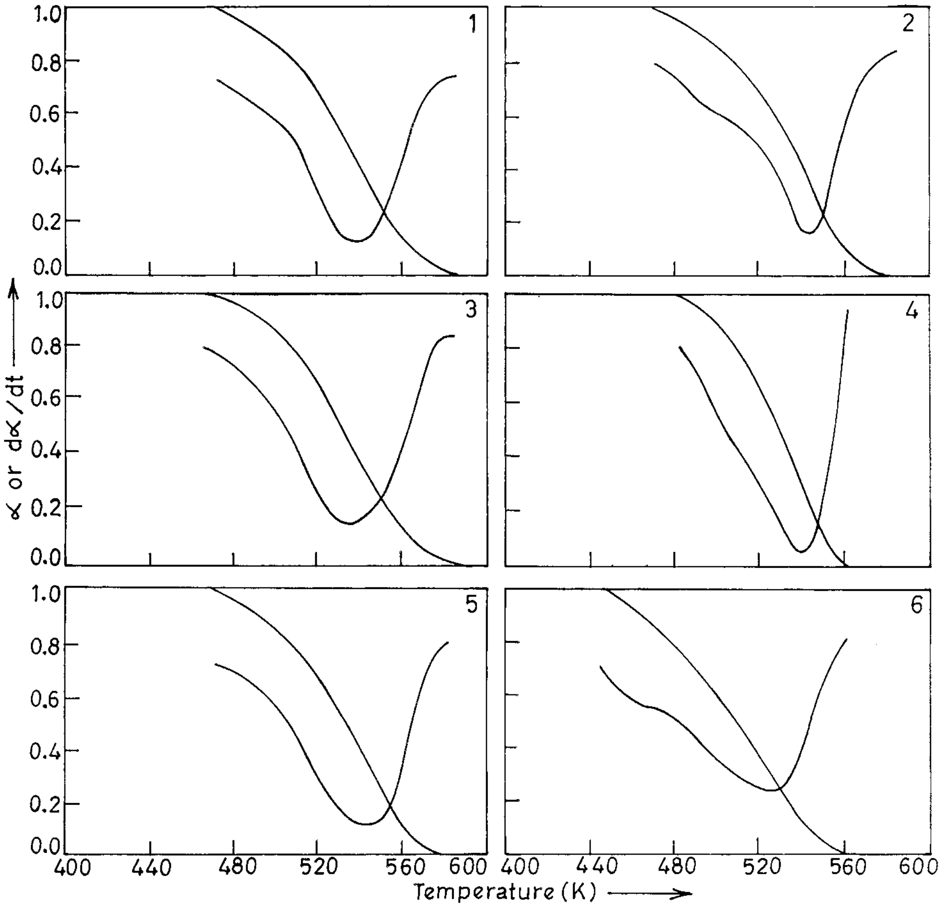

Fig. 3. Plots of ($d\alpha/dt$) vs. T for the first step for complexes 1–6.

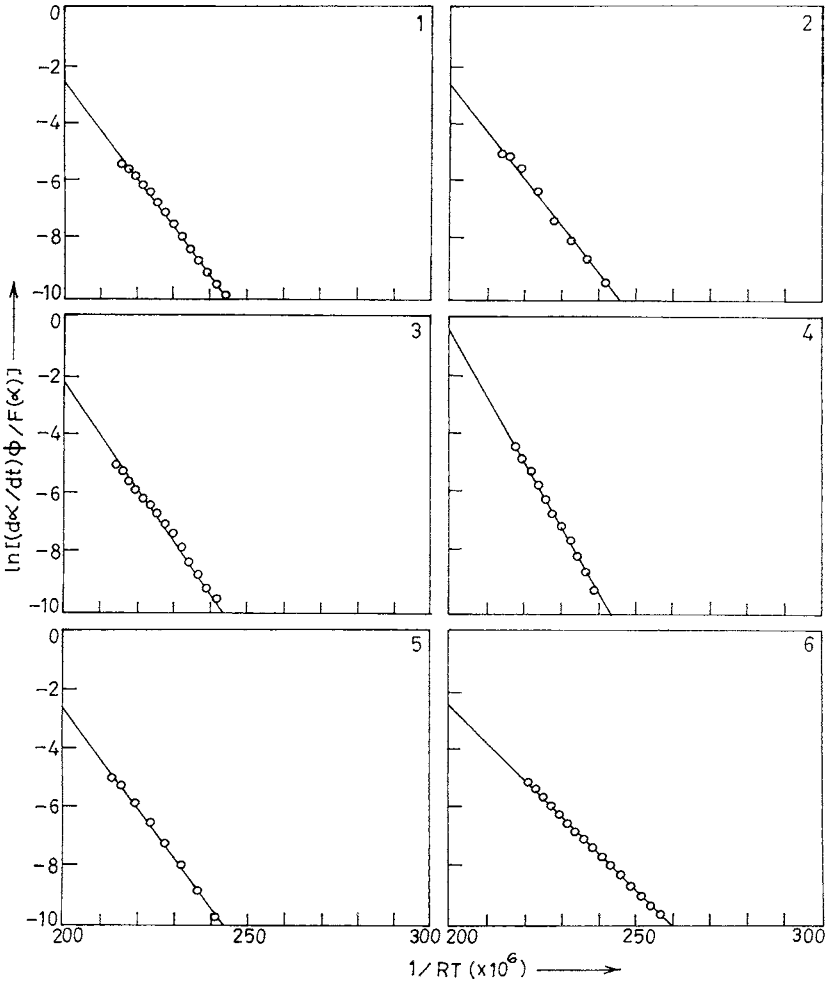

Fig. 4. Plots of ln[(dα/dt)/F(α)] vs. 1/RT for D_3 mechanistic model [$F(\alpha) = (3/2)(1-\alpha)^{2/3}/(1-(1-\alpha)^{1/3})$].

higher vis-à-vis those obtained using Freeman and Carrol method (Fig. 4).

The activation thermodynamic parameters, namely, enthalpy ($\Delta H^{\#}$), entropy ($\Delta S^{\#}$) and free energy ($\Delta G^{\#}$) were evaluated using standard equations and the values thus obtained are given in Table 4. The values of $\Delta S^{\#}$ were found to be negative but very small for all complexes. This indicates that the transition states for

Table 4
Decomposition rate constant and thermodynamic parameters for the thermal decomposition process at 500 K

Complex	$k \times 10^3$ (s^{-1})	$\Delta H^{\#}$ (kJ/mol)	$\Delta S^{\#}$ (J/K mol)	$\Delta G^{\#}$ (kJ/mol)
[Mn($S_2CCN)_2$]	1.252	109.79	−1.23	110.40
[Fe($S_2CCN)_2$]	1.263	59.45	−2.69	60.79
[Co($S_2CCN)_2$]	1.262	84.21	−1.97	85.20
[Ni($S_2CCN)_2$]	1.489	72.17	−2.24	73.29
[Cu($S_2CCN)_2$]	1.149	74.04	−2.28	75.18
[Zn($S_2CCN)_2$]	2.156	41.49	−3.14	43.06

these thermal decompositions are primarily intramolecular, removing CS_2 in a concerted step and thus do not exert any significant restriction on the vibrational degrees of freedom. However, the higher order observed for $[Mn(S_2CCN)_2]$ is suggestive of intermolecular interaction for the removal of C_3S_2 and is in agreement with the nature of the decomposition process.

References

[1] R.P. Burns, F.P. McCullough, C.A. McAuliffe, Adv. Inorg. Chem. Radiochem. 23 (1980) 211.

[2] D. Coucouvanis, Progr. Inorg. Chem. 26 (1979) 301.

[3] D. Coucouvanis, Progr. Inorg. Chem. 11 (1970) 233.

[4] R. Prasad, U.C. Agarwala, Bull. Chem. Soc. Jpn. 65 (1992) 3398.

[5] R. Prasad, U.C. Agarwala, Transition Met. Chem. 19 (1994) 390.

[6] D.M.A. Melo, F.M.M. Borges, F.J.S. Lima, H. Scatena Jr., L.B. Zinner, V.J. Fernandes Jr., W.S. C Souza, Z.R. Silva, J. Thermal Anal. Calorimet. 56 (1999) 805.

[7] H.E. Simmons, D.C. Blomstrom, R.D. Vest, J. Am. Chem. Soc. 88 (1962) 756.

[8] R.J. Pleus, H. Waden, W. Saak, D. Hasse, S. Pohl, J. Chem. Soc., Dalton Trans. (1999) 2601.

[9] G. Bahr, G. Schleitzer, Chem. Ber. 88 (1956) 1771.

[10] J. Bassett, R.C. Denny, G.H. Jeffery, J. Mendham, Vogel's Textbook of Quantitative Inorganic Analysis, ELBS/ Longman, New York, 1978.

[11] J.V. Rodrigues, I.C. Santos, V. Gama, R.T. Henriques, J.C. Waerenborgh, M.T. Duarte, M. Almerdu, J. Chem. Soc. Dalton Trans. (1994) 2655.

[12] S.I. Shupack, E. Billing, R.J.H. Clarke, R. Williams, H.B. Gray, J. Am. Chem. Soc. 86 (1964) 4594.

[13] V.M. Drager, G. Gattow, Z. Anorg. Allg. Chem. 387 (1972) 281.

[14] M. Maltese, J. Chem. Soc., Dalton Trans. (1972) 2664.

[15] R. Eisenberg, Progr. Inorg. Chem. 12 (1970) 294.

[16] G.A. Eisman, W.M. Reiff, Inorg. Chem. 20 (1981) 3481.

[17] B.W. Fitzsimmons, S.E. Al Mukhtar, L.F. Larkwortha, R.R. Patel, J. Chem. Soc., Dalton Trans. (1975) 1969.

[18] T.C. Woon, M.F. Mackay, M.J. O'Connor, Inorg. Chim. Acta 58 (1982) 5.

[19] M. Bonamico, G. Dessy, A. Mugnoli, A. Yaciago, L. Zambonells, Acta Crystrallogr. 19 (1965) 886.

[20] M. Martin, P.W.G. Newman, B.W. Robinson, A.H. White, J. Chem. Soc., Dalton Trans. (1972) 2223.

[21] W.W. Wendtlandt, Thermal Analysis, 2nd Edition, Wiley, New York, 1974, pp. 45–53.

[22] D. Dollimore, in: E.L. Charsley, S.B. Warrington (Eds.), Thermal Analysis Techniques and Applications, The Royal Society of Chemistry, London, 1992, p. 31.